Supporting Information

Realizing negative thermal expansion over an extended temperature range in $PbTiO_3$-based perovskites

Zhao Pan[1,*], Fengyi Zhou[2], Mengqi Ye[1], Duo Wang[2], Qiumin Liu[3], Takumi Nishikubo[4,3], Xubin Ye[1], Xiao Wang[1], Jin Liu[1], Nianpeng Lu[1], Shogo Kawaguchi[5], Masaki Azuma[3,4], Youwen Long[1,6,*]

[1]*Beijing National Laboratory for Condensed Matter Physics, Institute of Physics, Chinese Academy of Sciences, Beijing 100190, China*

[2]*Faculty of Applied Sciences, Macao Polytechnic University, Macao 999078, China*

[3]*Laboratory for Materials and Structures, Tokyo Institute of Technology, Yokohama 226-8503, Japan*

[4]*Kanagawa Institute of Industrial Science and Technology (KISTEC), Kanagawa 243-0435, Japan*

[5]*Research and Utilization Division, Japan Synchrotron Radiation Research Institute (JASRI), Hyōgo 679-5198, Japan*

[6]*Songshan Lake Materials Laboratory, Dongguan, Guangdong 523808, China*

Corresponding authors:

E-mail: Z. Pan, zhaopan@iphy.ac.cn;

Y. Long, ywlong@iphy.ac.cn

Received: January 15, 2025; Revised: May 16, 2025; Accepted: May 19, 2025

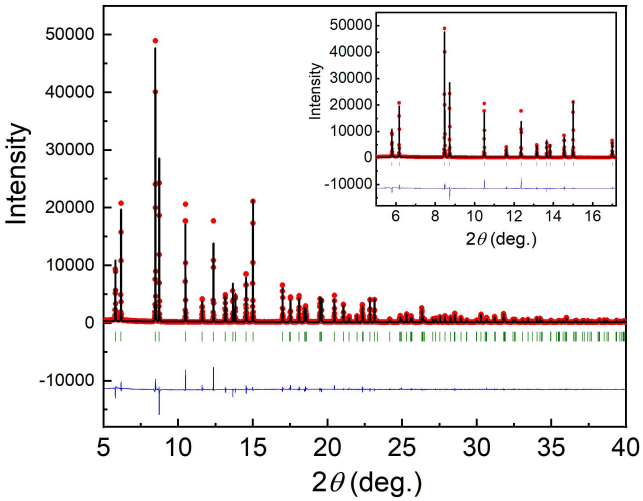

Figure S1. Rietveld full profile refinement of SXRD patterns of pristine PT at room temperature. Observed (red, solid circles), calculated (black line), and their difference profiles (bottom line) are shown. The Bragg reflection positions are indicated by the green ticks.

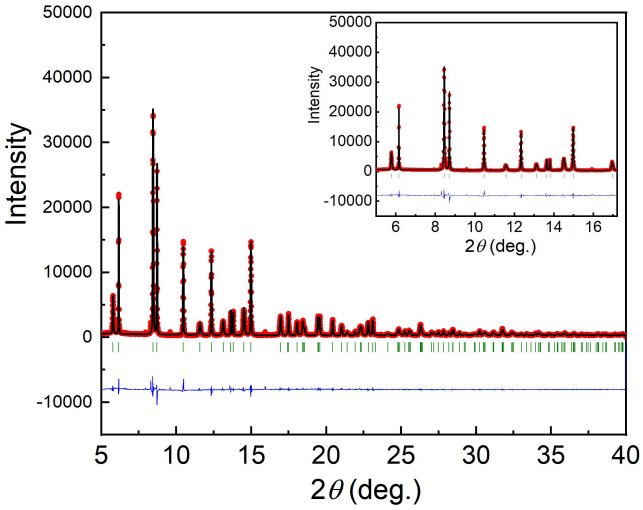

Figure S2. Rietveld full profile refinement of SXRD patterns of tetragonal 0.95PT-0.05BY at room temperature. Observed (red, solid circles), calculated (black line), and their difference profiles (bottom line) are shown. The Bragg reflection positions are indicated by the green ticks.

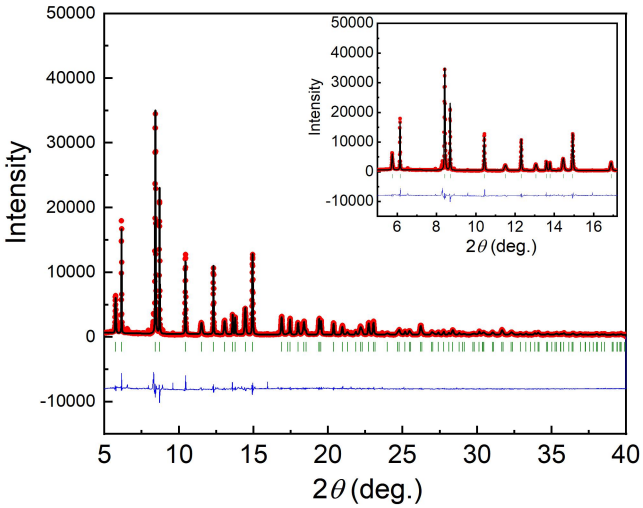

Figure S3. Rietveld full profile refinement of SXRD patterns of tetragonal 0.90PT-0.10BY at room temperature. Observed (red, solid circles), calculated (black line), and their difference profiles (bottom line) are shown. The Bragg reflection positions are indicated by the green ticks.

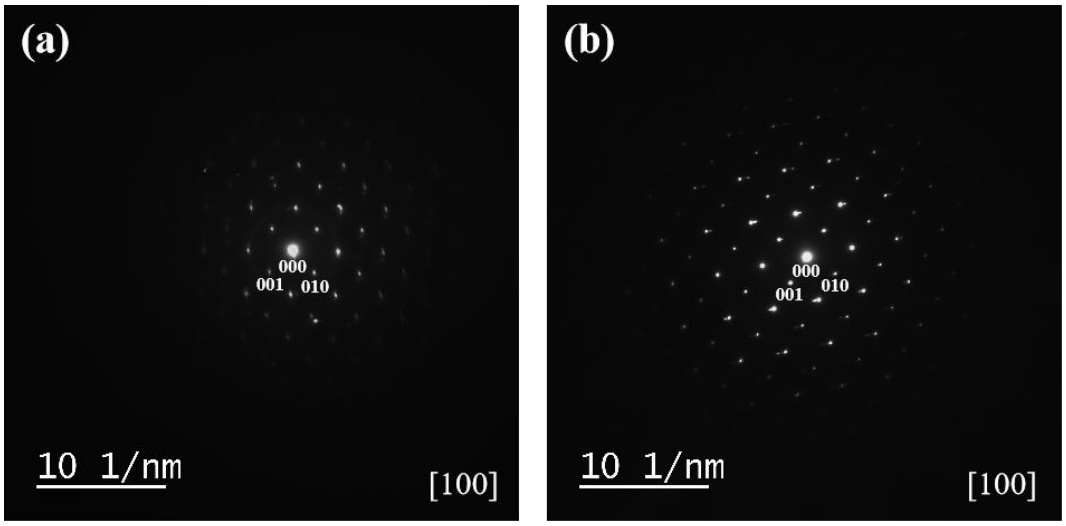

Figure S4. The SAED patterns of the (1-*x*)PT-*x*BY (*x* = 0.05 and 0.10) compounds along the [100] zone axis.

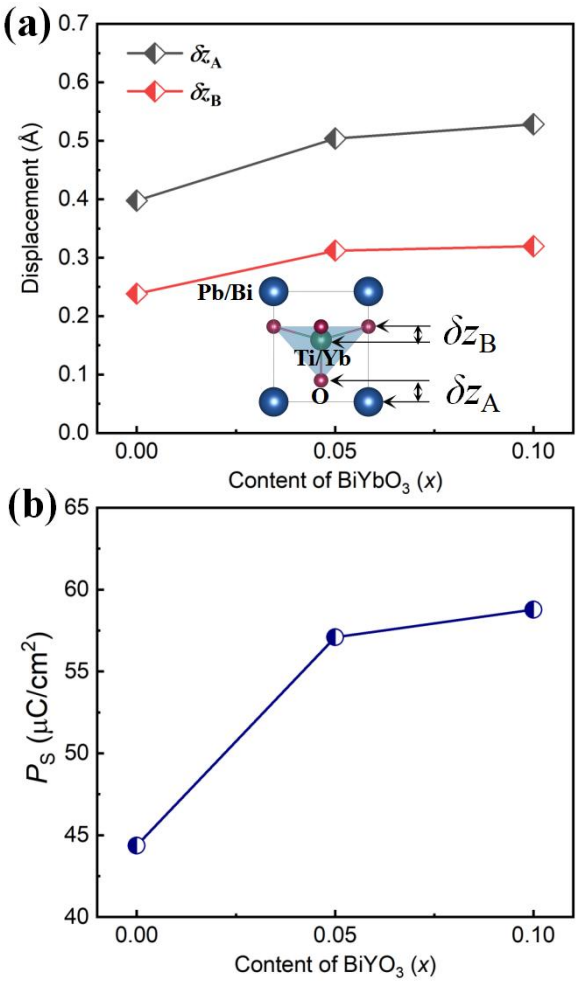

Figure S5. (a) P_S displacement of δz_A and δz_B, and (b) the calculated spontaneous polarization of of (1-x)PT-xBY as a function of x. The inset is the schematic diagram of P_S. The error bars are smaller than the symbols.

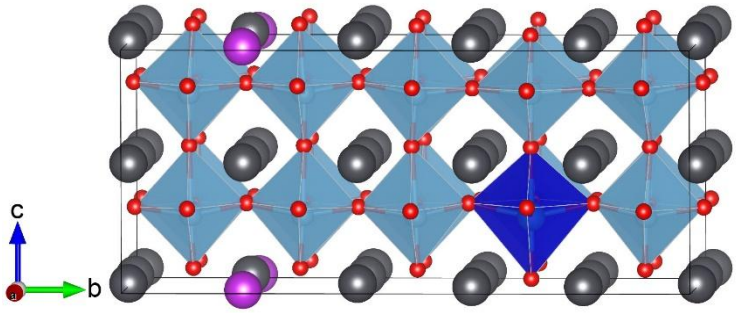

Figure S6. Optimized 0.95PT-0.05BY structural model with a 2 × 5 × 2 supercell. Gray, purple, blue, light blue and red spheres represent Pb, Bi, Yb, Ti and O atoms.

We have further examined the effect of functional choice – specifically, PBE, PBEsol, LDA, and the SCAN meta-GGA – on both aspects of the parent compound, $PbTiO_3$, as detailed below. The accuracy of the obtained crystal structure is examined by performing both full geometry optimization (ISIF = 3) and internal atomic relaxation with the lattice parameters constrained to experimental values (ISIF = 2) using the VASP code. The electronic structure is subsequently evaluated through a self-consistent calculation based on the corresponding relaxed structure.

As illustrated in Figure S7, the choice of exchange-correlation functionals in the simulations leads to slight variations in the *a*-axis lattice parameter, and noticeable changes in the *c*-axis, which in turn result in noticeable modifications to the *c/a* ratio and local Ti-O bond lengths. Specifically, among the four functionals considered, SCAN meta-GGA and PBE overestimate the experimental c-axis value by 2.9% and 11.2%, respectively, resulting in longer l_1 bonds. Whereas the other two functionals underestimate the c-axis by 1.5% and 2.8%, leading to shorter l_1 bonds. These results are consistent with those reported in [1]. Since the lattice deviation associated with the PBE functional is relatively large, it is not suitable for fully relaxing the crystal structure. On the other hand, for simulations using fixed experimental lattice parameters, the resulting atomic displacements are highly consistent across all functionals, with the maximum deviation both l_1 and l_3 is within 0.02 Å, as shown in Figure S8. This confirms that, by using the PBE functional in combination with internal atomic relaxation only – the approach adopted in our manuscript – yields atomic positions with sufficiently high accuracy.

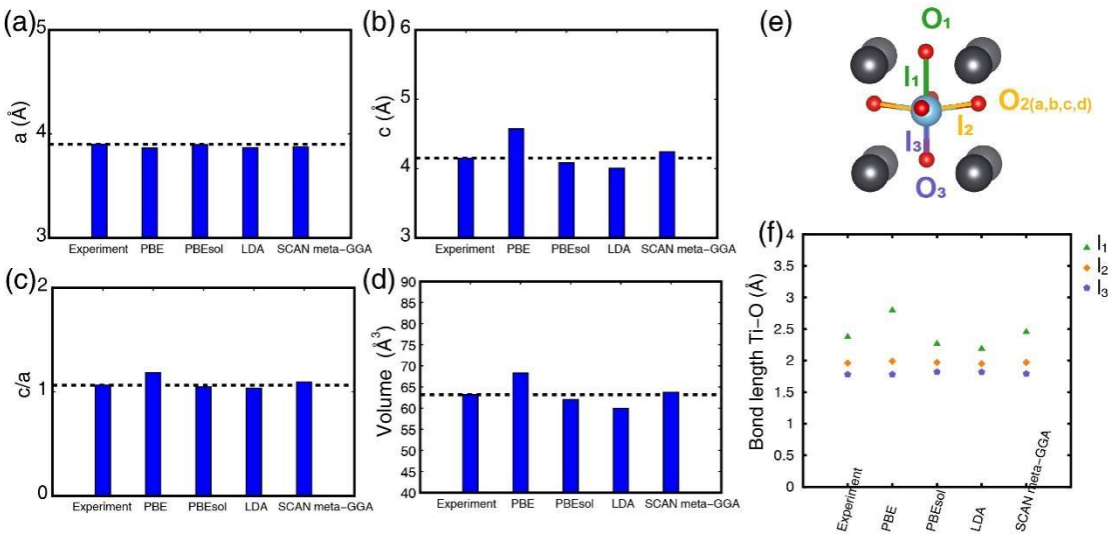

Figure S7. Lattice parameters of (a) *a*, (b) *c*, (c) *c/a*, (d) volume. (e) Structural model and (f) Ti-O bond lengths of the fully optimized $PbTiO_3$ structure.

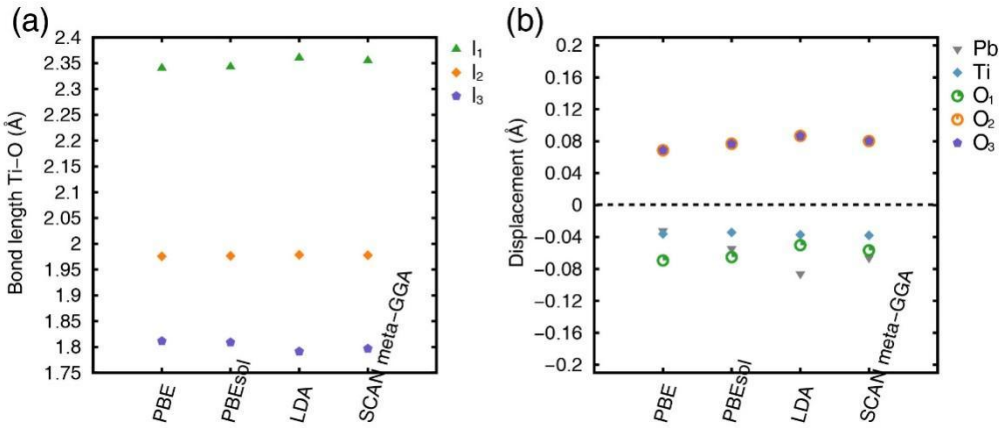

Figure S8. (a) Bond length of Ti-O and (b) displacement of various atoms based on the optimization with fixed lattice.

In addition to the crystal structure, the functional dependence of the electronic structure is further analyzed based on the optimized structures obtained above. Take the electronic DOS as an example (Figure S9), for the occupied states, the DOS spectra obtained from all functionals are nearly identical. As for the unoccupied states, three of the functionals yield similar results, while the SCAN meta-GGA shifts the overall unoccupied states upward by approximately 0.4 eV. Given that our theoretical work focuses only on the ground state of the compound, and that there is no compelling evidence that the SCAN meta-GGA yields a considerably better description of the electronic structure in similar systems, we consider the PBE functional to be sufficiently accurate for capturing the electronic properties in this study.

In summary, based on a comprehensive assessment of different exchange-correlation functionals for this system, we conclude that combining partial geometry optimization with the PBE functional yields sufficiently accurate results for reliably describing both the atomic displacements and the electronic structure.

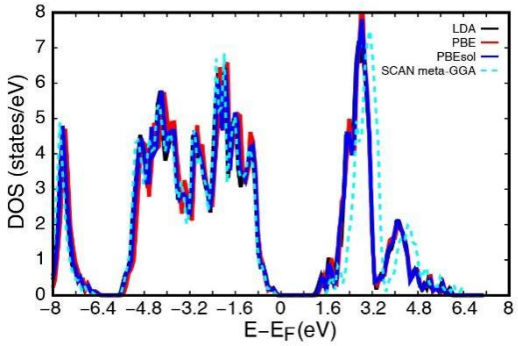

Figure S9. DOS for the optimization structure with lattice fixed and atoms relaxation.

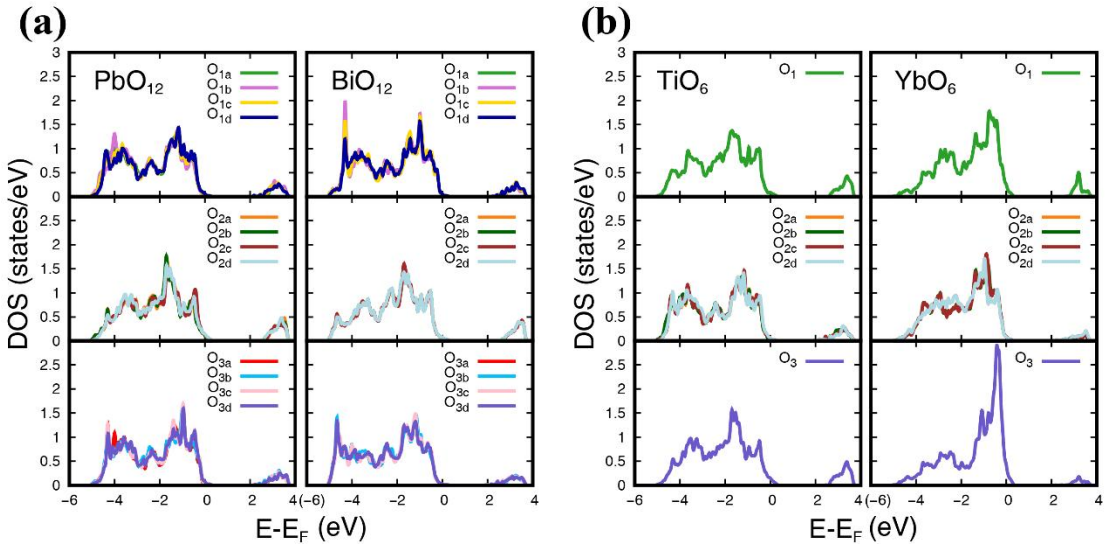

Figure S10. Calculated density of states (DOS) in the local (a) AO_{12} and (b) BO_6 environment. DOSs from three different types of O atoms with varying bond lengths are plotted in the upper (l_1), middle (l_2), and lower (l_3) panels.

Table S1. Refined structural parameters of the (1-*x*)PT-*x*BY (*x* = 0, 0.05, and 0.10) compounds at room temperature.

Composition	Space group	Atom	Site	*g*	*x*	*y*	*z*	*B* (Å^2)	Cell (Å)	*R* (%)
x = 0	*P*4*mm*	Pb	1a	1	0	0	0	0.74(4)		
		Ti	1b	1	0.5	0.5	0.5383(7)	0.53(6)	*a* = 3.9006(9)	R_{wp} = 12.9
		O1	1b	1	0.5	0.5	0.1100(7)	1	*c* = 4.1517(0)	R_p = 9.82
		O2	2c	1	0.5	0	0.5886(8)	1		
x = 0.05	*P*4*mm*	Pb	1a	0.95	0	0	0	0.75(3)		
		Bi	1a	0.05	0	0	0	0.75(3)		
		Ti	1b	0.95	0.5	0.5	0.5460(2)	0.77(5)	*a* = 3.9071(3)	R_{wp} = 9.64
		Yb	1b	0.05	0.5	0.5	0.5460(2)	0.77(5)	*c* = 4.1638(6)	Rp = 6.91
		O1	1b	1	0.5	0.5	0.1070(3)	0.58(9)		
		O2	2c	1	0.5	0	0.6279(3)	0.58(9)		
x = 0.10	*P*4*mm*	Pb	1a	0.9	0	0	0	0.7844(9)		
		Bi	1a	0.1	0	0	0	0.7844(9)		
		Ti	1b	0.9	0.5	0.5	0.5497(5)	1.0652(1)	*a* = 3.9161(4)	Rwp = 12.2
		Yb	1b	0.1	0.5	0.5	0.5497(5)	1.0652(1)	*c* = 4.1877(5)	Rp = 8.06
		O1	1b	1	0.5	0.5	0.1091(2)	1.1512(1)		
		O2	2c	1	0.5	0	0.6346(10)	1.1512(1)		

Table S2. The interatomic distance of the (1-*x*)PT-*x*BY (*x* = 0, 0.05, and 0.10) compounds at room temperature.

Distance (Å)	*x* = 0	*x* = 0.05	*x* = 0.10
Ti(Yb)-O1 (long)	2.374(9)	2.336(7)	2.299(9)
Ti(Yb)-O2 (×4)	1.9616(14)	1.9831(8)	1.9899(11)
Ti(Yb)-O3 (short)	1.778(9)	1.828(7)	1.888(9)
Pb(Bi)-O1	2.7958(14)	2.7985(10)	2.8000(12)
Pb(Bi)-O2	2.591(8)	2.493(3)	2.485(3)
Pb(Bi)-O3	3.128(10)	2.493(3)	2.485(3)

Table S3. Calculated bond lengths in the ground state AO_{12} and BO_6 structures.

Bonds	AO_{12} (Å)		BO_6 (Å)	
	PbO_{12}	BiO_{12}	TiO_6	YbO_6
l_1	3.27	3.40	2.34	2.37
l_2	2.76	2.75	1.98	2.17
l_3	2.51	2.32	1.81	2.14

References

[1] Zhang Y, Sun J, Perdew JP, et al. Comparative first-principles studies of prototypical ferroelectric materials by LDA, GGA, and SCAN meta-GGA. *Phys Rev B*, 2017, **96**: 035143.